CrossMark
click for updates

# Green synthesis and *in silico* characterization of 4-Hydroxy-3-methoxybenzaldehyde Schiff bases for insulysin inhibition – a potential lead for type 2 diabetes mellitus

Sridevi Chigurupati[1]* iD, Vasanth Raj Palanimuthu[2], Suganya Kanagaraj[3], Sumathi Sundaravadivelu[3],
Venkata Ramaiah Varadharajula[4] iD

[1]Department of Medicinal Chemistry and Pharmacognosy, College of Pharmacy, Qassim University, Buraidah, Kingdom of Saudi Arabia.
[2]Department of Pharmaceutical Biotechnology, JSS College of Pharmacy, JSS Academy of Higher Education & Research, Ooty, Nilgiris, TN, India.
[3]Department of Biochemistry, Biotechnology and Bioinformatics Avinashilingam Institute for Home Science and Higher Education for Women, Tatabad Forest College Campus, Coimbatore, India.
[4]Department of Dental Hygiene, College of Applied Health Sciences in Alrass, Qassim University, Al-Rass Region, Saudi Arabia.

## ARTICLE INFO

## ABSTRACT

The global prevalence of diabetes is likely to increase sharply from 171 million in 2000 and 366 million in 2030. This clearly depicts the frailty of the existing medication for treating diabetes. Organic compounds, especially Schiff bases, flaunt anti-diabetic effects specifically for type 2 diabetes mellitus (T2DM). The research work demonstrates the synthesis of 4-Hydroxy-3-methoxybenzaldehyde Schiff bases following green chemistry and substantiates its activity against T2DM using *in silico* methods. All the three Schiff bases provide evidence for insulysin inhibition with Pa values more than 0.6 with strict adherence to Lipinski's rule. Insulysin or insulin-degrading enzyme is a zinc metalloprotease involved in the degradation of insulin and is signified to be a diabetes susceptibility gene. Molecular docking studies with the synthesized Schiff bases against insulysin (3E4A) reveal that compounds S2 and S3 exhibit better binding and affinity than the natural inhibitor ML345.

## INTRODUCTION

The global prevalence of diabetes is likely to increase sharply from 171 million in 2000 and 366 million in 2030 (Wild *et al*., 2004). The increase in diabetes has been witnessed in all regions of the world (Hardling *et al*., 2019) and confirms continuity of the "diabetes crisis" (Ampofo and Boateng, 2020). The World Health Organization projects that diabetes will be the 7th leading cause of death in 2030 (Mathers *et al*., 2006). Diabetes is one of the leading causes for renal failure, visual disability, and progressive loss of vision, heart diseases, vascular and neurological disease processes manifested as diabetic foot disease which leads to

amputation (Chigurupati *et al*., 2019; Gaidhane *et al*., 2017). There is now ample evidence that it is possible to avoid type 2 diabetes (which accounts for over 90% of diabetes worldwide) (Dagogo-Jack, 2017). Due to the gradual degradation of beta-cell function during type 2 diabetes mellitus (T2DM), insulin therapy will eventually be needed in many patients with long-standing T2DM. Insulin, a biologically important insulin-degrading enzyme (IDE) substrate, has pleiotropic roles, including the regulation of the metabolism of carbohydrates, lipids, and amino acids; the primary causes of T2DM are aberrant insulin levels and improper responses to insulin and other glucose-controlled hormones, with one of its hallmarks being glucose intolerance (Prentki and Nolan, 2006). Insulin has a short half-life in circulation, presumably because of the clearance mechanism's highly efficient action, such as receptor-mediated internalization and IDE degradation (Farris *et al*., 2004).

For a long time, insulin degeneration was not considered imperative for insulin regulation. Be that as it may, insulin

*Corresponding Author
Sridevi Chigurupati, Department of Medicinal Chemistry and Pharmacognosy, College of Pharmacy, Qassim University, Buraidah, Kingdom of Saudi Arabia. E-mail: sridevi.phd @ gmail.com*

degeneration is now related to the regulation of insulin and the onset of type 2 diabetes (Leissring *et al.*, 2010). As early as 1949, IDE was discovered and its name is coined based on its ability to bind insulin and rapidly causing its catabolism. Subsequently, IDE was proven to inactivate other small proteins of amyloidogenic peptides besides insulin, namely amylin, glucagon, and also the 29-residue peptide hormone, glucagon in glucose homeostasis (proteostasis), that depend on the complex interplay of these hormones (Gilbert, 2014). IDE's role in insulin clearance indicates that IDE inhibitors could be used in patients with T2DM to modulate insulin levels (Ye, 2013).

Insulysin is an evolutionarily preserved zinc metalloprotease that cleaves and inactivates several bioactive peptides with different sequences and structures, thus preventing peptide aggregates from forming in several subcellular compartments. Without influencing the catabolism of other IDE substrates, such as glucagon, the optimal IDE inhibitor to treat T2DM could preferentially decrease the clearance of insulin and amylin. Mirsky and Perisutti (1955) stated six decades ago that an endogenous liver-insulated IDE inhibitor could boost the hypoglycemic action of insulin in rats and rabbits, highlighting the possible use of IDE inhibitors to modulate insulin action (Morris *et al.*, 2009). The molecular basis for IDE-mediated degradation of amyloidogenic peptides was discovered by structural and biochemical studies, and this knowledge was exploited to establish promising IDE inhibitors to improve homeostasis of glucose. Consistent with the fact that IDE defects contribute to the intolerance of age-dependent glucose and are associated with T2DM, binding sites away from the catalytic cleft are IDE inhibitors that elicit improved glucose tolerance (Berman *et al.*, 2000). Despite the fact that the idea has been put forward for more than a few years, the discovery of insulysin inhibitors is still progressing (Lipinski, 2004).

The aphorism 'an ounce of prevention is worth a pound of cure' is at the root of the theory, one of green chemistry's 12 principles, a systematic collection of designs that have driven the growth of green chemistry for many years. The cost of storing, treating, and disposing of dangerous chemicals is so high that progress is inevitably suppressed: funds must be redirected to hazard management from research and development (Chigurupati *et al.*, 2017). The creation of environmentally friendly benign approaches for the synthesis of Schiff bases (green chemistry), high-yielding and safe approaches, remains a highly desired objective in chemistry (Blakemore *et al.*, 2018). Schiff bases appear as a standout (Manolopoulou *et al.*, 2009) among the most commonly used organic compounds, among which Schiff bases of 4-Hydroxy-3-methoxybenzaldehyde (I, vanillin) have been used in organic synthesis and polymer stabilizers for various purposes, such as catalysts and intermediates. Studies have shown that the Schiff base derivative possesses activities including anti-inflammatory, anti-proliferative, anti-malarial, anti-fungal, and anti-bacterial properties (Durham *et al.*, 2015). It has been proven that Schiff bases are biologically active due to the presence of the azomethine (NHN=CH-) moiety in their chemical structure. Schiff bases derivative from I were extensively subjected to research due to the peculiarity in forming complexes with metals like copper, which is being synthetically flexible, sensitive, and selective (Tabassum *et al.*, 2013).

These facts from various literature sources on the importance of Schiff bases encouraged us to synthesize Schiff bases by using the green synthesis technique with ethanol as the green solvent and evaluate its potential as an anti-diabetic agent, should it possess the insulysin inhibiting property. This study has characterized the three synthesized Schiff bases derivatives as insulysin inhibitors whose inhibitory effect was tested through *in silico* docking studies.

## METHODOLOGY

### Green synthesis Schiff bases of 4-Hydroxy-3-methoxybenzaldehyde (S1–S3)

The solid starting materials, 4-Hydroxy-3-methoxybenzaldehyde, and aromatic amines were finely powdered. Initially, a mixture of 4-Hydroxy-3-mehtoxybenzaldehyde (2.5 mmol) and aromatic amine (2.5 mmol) were dissolved in 5 ml of ethanol at room temperature until completely dissolved. The solution was then triturated for a specified time to yield 4-Hydroxy-3-methoxybenzaldehyde Schiff bases. A base catalyst triethylamine (0.01 mmol) was then added during trituration and the chemical reaction is illustrated in Figure 1. Filtration of the solution retained the filtrate of crystalline product which was then washed with water and recrystallized using (1:5) $H_2O$: $C_2H_5OH$ (Bendale *et al.*, 2011).

### Spectroscopical analysis

The UV-visible absorption spectra are obtained in methanol at room temperature and the absorption range in the 200–400 nm region was fixed for analysis. Fourier-transform infrared spectroscopy (FTIR) identifies chemical bonds in a molecule by producing an infrared absorption spectrum. The spectra produced a profile of the sample, a distinctive molecular fingerprint that can be used to screen and scan samples for many different components. The FTIR is an effective analytical instrument for detecting functional groups and characterizing covalent bonding information. The FTIR spectra were carried out by embedding samples in KBr pellets and absorption measured in the range of 4,000–400 cm$^{-1}$. Proton nuclear magnetic resonance spectroscopy ($^1$H-NMR) was carried out to identify hydrogen-1 nuclei within the molecules of a substance, to determine the structure of its molecules. $CdCl_3$ was used as a solvent and tetramethylsilane (TMS) was used as an internal standard. The proton NMR spectra are characterized by chemical shifts ($\delta$) in the range 14–1 ppm.

### Chromatographic analysis

The thin layer chromatography technique, using benzene: pyridine: ammonia (8:2:1) as solvent system, allowed the completion of the reaction to be confirmed using $R_f$. The spots are visualized by using the UV chamber. The crystalline powder was then dried and further kept in a desiccator to protect the product from atmospheric moisture.

### Molecular docking analysis

The receptor for the docking was retrieved from the Protein Data Bank (Berman *et al.*, 2000). Molecular docking of the identified receptor and synthesized ligands was carried out using AutoDock Tools (ADT) 1.5.6. by employing the methods below.

**Preparation of receptor and ligand files**

To determine the binding affinity between them, AutoDock contains both receptor and ligand in the Protein data bank with partial charges Q and T. (PDBQT) format. Atomic coordinates, partial charges, and atom forms are limited by the PDBQT format. Initially, the AutoDock workspace accessed the receptor file in PDB format obtained from the Protein Data Bank. The molecules of water in the receptor file have been extracted and tacit hydrogen atoms have been inserted. Finally, partial fees were introduced and the PDBQT format of the receptor file was saved. Likewise, AutoDock downloaded the ligand files in the PDB format and saved them in the PDBQT format.

**Preparation of grid and dock parameter files**

For the grid calculation, the AutoGrid 4.2 software in ADT was used. The grips map was oriented along the ligand binding site with a 90 × 90 × 90 scale and spacing of 0.375 Å. In order to run the AutoGrid program, the receptor and ligand files in PDBQT format along with the matrix maps were saved as the grid parameter file. The AutoDock parameter file with receptor, ligand, and selection of AutoDock parameters was generated after AutoGrid calculation.

**Docking and visualization**

Docking was carried out on the receptor binding site using the Lamarckian Genetic Algorithm with 10 independent runs per ligand with an initial population of 150 randomly positioned ligands. For $27 \times 10^3$ generations, a maximum of $2.5 \times 10^5$ energy assessments were carried out with a mutation rate of 0.02 and a cross-over rate of 0.80. For 6% of the population, the local energy minimization algorithm was limited to 100 steps. The overall translation steps were set at 0.2 Å to explore the conformational space of ligands, and the overall rotation and torsion rotation stage in the docking studies was set at 5. In ADT, the AutoDock 4.0 program was introduced and the docking scores were recorded in kcal/mol using binding free energy energies. Using Pymol, the bound complex was visualized with the receptor and ligand.

**Biological activity analysis**

The chemical structures for the ligand molecules were created in mol format using ACD Lab's Chemsketch (www. ACDlabs.com). The created files were then evaluated for their biological activity using predictions of activity spectra for the biologically active substances (PAAS) server (Neelakantan *et al.*, 2010). The biological activity spectrum denotes the property of a compound depending on its structure and physicochemical properties. PAAS predicts this activity through Structure activity relationship. (SAR) analysis with a training set of more than 35,000 compounds and 500 different types of biological activity. PAAS predicts the probability of the compound to be active ("Pa") or inactive ("Pi") along with the biological activity of the compound. The synthesized ligands were assessed for compliance
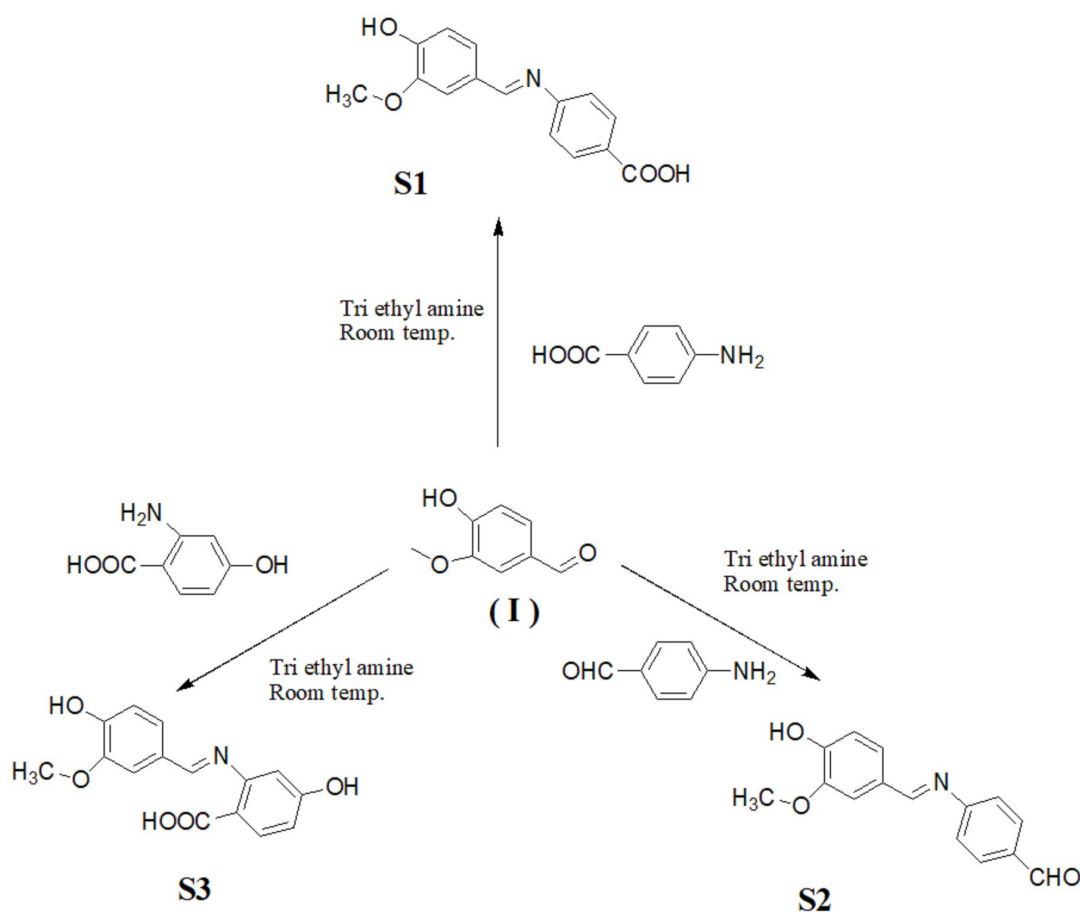


**Figure 1.** Green synthesis of 4-Hydroxy-3-methoxybenzaldehyde Schiff bases (S1–S3).

with Pfizer's or Lipinski's rule of five using the Molsoft web server (http://molsoft.com/mprop/) to evaluate the drug-likeness of a chemical compound (Lipinski, 2004). Since insulysin inhibitors can hold key for the treatment of type 2 diabetes, the synthesized compounds were tested for their drug-like properties using the Molinspiration Webserver (Leissring *et al.*, 2010).

## RESULTS AND DISCUSSION

### Green synthesis Schiff bases of 4-Hydroxy-3-methoxybenzaldehyde (S1–S3)

The yield and melting points of 4-Hydroxy-3-methoxybenzaldehyde Schiff bases are given in Table 2.

### UV and NMR Spectral Data for 4-Hydroxy-3-methoxybenzaldehyde Schiff bases (S1–S3)

The UV and $^1$H NMR spectral data of 4-Hydroxy-3-methoxybenzaldehyde derivative are tabulated in Table 1. The UV-visible absorption spectra are obtained in methanol at room temperature. The compounds exhibit intense bands in the 200–400 nm region, and the bands at the 290–350 nm range involve π→π* transitions of the C=N group. The IR spectra of the Schiff bases show medium or strong intensity absorption bands at 1,625–1,650 cm$^{-1}$ assigned to the C=N stretching mode. The presence of aromatic rings has been identified by their characteristic ring vibrations at 1,500–1,400, 1,100–1,050, and 900–700 cm$^{-1}$ regions. The absence of bands, characteristic of ν(C=O) and primary amine ν(NH), confirms the formation of the proposed Schiff base framework. Methoxy and CH=N groups stretching vibrations appear between 3,000 and 2,800 cm$^{-1}$. From the $^1$H NMR spectral data there is a doublet observed at 8.40 indicating the benzylidenimin formation. The physical properties of 4-Hydroxy-3-methoxybenzaldehyde derivatives are shown in Table 2.

### Molecular docking analysis

The three compounds S1, S2, and S3 were docked with the receptor insulysin which was retrieved from PDB (PDB Id 3E4A). An inhibitor of insulysin ML345, which was retrieved

from Pubchem (CID: 57390068), is shown in Figure 2 and retained as the standard for the docking studies. Table 3 portrays the binding energies of the different poses of the ligands bound to the receptors. Ligand S1 shows the maximum binding free energy among the other ligands, as well as the standard. The average binding free energy of ligand S1 is −4.86 ± 0.37 kcal/mol. But the binding free energies of the other two ligands S2 and S3 demonstrate an average of −5.97 ± 0.64 and −5.73 ± 0.64 kcal/mol. Much to our attention, ligands S2 and S3 possess minimum binding free energies than the reported inhibitor (ML345), reflecting a better binding affinity for ligands S2 and S3 than ML345. The binding modes of the different ligands are shown in Figure 3. Table 4 depicts the inhibitory constant for the different poses of the receptor ligand complex, which is an indication of the potency of an inhibitor. It is obvious from the table that the ligands, as well as ML345, show a very
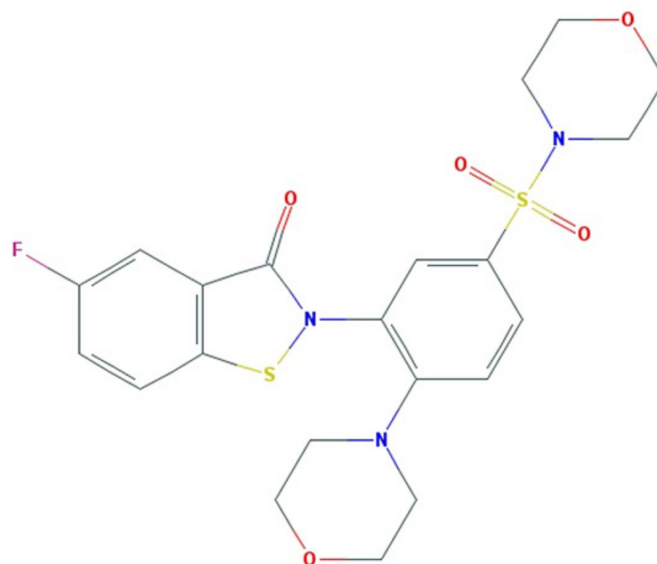


**Figure 2.** Molecular structure of ML345.

**Table 1.** Spectral data of 4-Hydroxy-3-methoxybenzaldehyde derivatives.

| S. No | Comp | UV λmax (nm) | $^1$H-NMR (CdCl$_3$/TMS) δ ppm | IR spectra frequency (cm$^{-1}$), KBr pellets |
|---|---|---|---|---|
| 1. | S1 | 296 | 6.50–8.54 (m, 7H, phenyl), 5.00 (second, 1H, hydroxy), 3.73 (second, 3H,-methoxy), 8.42 (day, 1H, benzylidenimin), 11.00 (second, 1H, carboxylic acid). | 3,670 (broad O-H str, phenolic), 3,056–3,020(Ar-H Str), 1,045 (C-O-C Str, phenyl methoxy), 1,645 (C=N Str, Azomethine) |
| 2. | S2 | 335 | 6.60–6.90 (m, 7H, phenyl), 5.00 (second, 1H, hydroxy), 9.60 (second, 1H, -CHO), 3.73 (second, 3H,-methoxy), 8.40 (day, 1H, benzylidenimin). | 3,598 (broad O-H str, phenolic), 3,050–3,030(Ar-H Str), 1,045 (C-O-C Str, phenyl methoxy), 1,645 (C=N Str, Azomethine); 1,700 (C=O Str, aldehyde) |
| 3. | S3 | 318 | 6.70–7.54 (m, 6H, phenyl), 5.00 (second, 2H, hydroxy), 3.73 (second, 3H,-methoxy), 8.43 (day, 1H, benzylidenimin), 11.00 (second, 1H, carboxylic acid). | 3,595 (broad O-H str, phenolic), 1,760 (C=O Str, COOH), 2,700 (O-H Str, COOH), 3,050–3,020(Ar-H Str), 1,045 (C-O-C Str, phenyl methoxy), 1,645 (C=N Str, Azomethine) |

**Table 2.** Physical data of 4-Hydroxy-3-methoxybenzaldehyde derivatives.

| Comp. | Reactant | Mol. formula of products | Mp/°C | Time/minute (product formation) | % yield | $R_f$ value |
|---|---|---|---|---|---|---|
| S1 | 4-aminobenzoic acid | $C_{15}H_{13}NO_4$ | 156-159 | 30 | 60 | 0.6 |
| S2 | 4-aminobenzaldehyde | $C_{15}H_{13}NO_3$ | 140-143 | 25 | 75 | 0.7 |
| S3 | 2-amino-4-hydroxy benzoic acid | $C_{15}H_{13}NO_5$ | 109-112 | 20 | 78 | 0.6 |

**Table 3.** Binding energies of the compounds based on their rank.

| Compounds | Binding energies for different poses ranked by energy (Kcal/mol) | | | | | | | | | | | |
|---|---|---|---|---|---|---|---|---|---|---|---|---|
| | 1 | 2 | 3 | 4 | 5 | 6 | 7 | 8 | 9 | 10 | Mean | SD |
| S1 | −5.4 | −5.29 | −5.11 | −5.02 | −4.96 | −4.92 | −4.71 | −4.57 | −4.34 | −4.33 | −4.86 | 0.37 |
| S2 | −6.97 | −6.81 | −6.53 | −6.13 | −6.02 | −5.9 | −5.56 | −5.36 | −5.31 | −5.12 | −5.97 | 0.64 |
| S3 | −6.92 | −6.43 | −6.02 | −5.82 | −5.72 | −5.71 | −5.69 | −5.34 | −5.04 | −4.65 | −5.73 | 0.64 |
| ML345 | −6.54 | −6.14 | −5.83 | −5.78 | −5.66 | −5.61 | −5.11 | −4.9 | −4.64 | −4.22 | −5.44 | 0.71 |
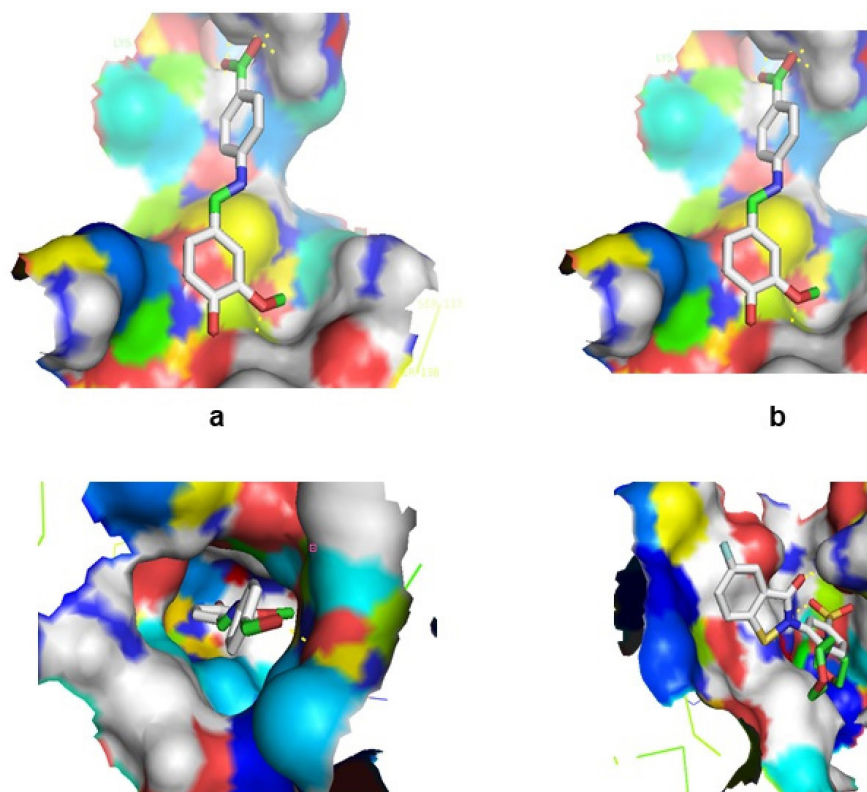


**Figure 3.** The binding modes of the different ligands with molecular surface representation of insulysin (a: Ligand S1; b: Ligand S2; c: Ligand S3; d: ML345).

**Table 4.** Inhibition constant of the compounds based on their rank.

| Compounds | Inhibition constant for different poses ranked by energy (μM) | | | | | | | | | | | |
|---|---|---|---|---|---|---|---|---|---|---|---|---|
| | 1 | 2 | 3 | 4 | 5 | 6 | 7 | 8 | 9 | 10 | Mean | SD |
| S1 | 109.82 | 132.99 | 178.34 | 210.18 | 243.48 | 248.5 | 353.78 | 443.99 | 658.79 | 673.8 | 325.36 | 205.05 |
| S2 | 7.8 | 10.22 | 16.36 | 31.87 | 38.38 | 46.97 | 84.34 | 117.49 | 127.89 | 177.63 | 65.89 | 58.24 |
| S3 | 8.52 | 19.49 | 38.56 | 54.03 | 64.69 | 65.25 | 67.6 | 122.24 | 202.75 | 391.16 | 103.429 | 115.44 |
| ML345 | 15.99 | 31.44 | 53.72 | 58.0 | 70.51 | 77.34 | 178.64 | 255.64 | 394.59 | 812.78 | 194.865 | 247.72 |

low Inhibitory constant in the range of 7.8–812.78 μM. But ligand S2 shows the least inhibitory constant of 65.89 ± 58.24 μM. Similarly, ligand S3 demonstrates an inhibitory constant of 103.429 ± 115.44 μM. Both these ligands enclose a lower inhibitory constant as compared to ML345. On the other hand, ligand S1 exerts an inhibitory constant of 325.36 ± 205.05 μM which is higher than ML345.

The intermolecular energy, which is the energy between atoms of different molecules of the docking between the receptor and different ligands, are presented in Table 5. The intermolecular energy for S1 falls within the range of −0.59 to −5.52 kcal/mol with a mean of −4.85 kcal/mol. Similarly, ML345 also exhibited an intermolecular energy of −4.05 kcal/mol in average. However, both ligands S2 and S3 portrayed a much lower intermolecular

**Table 5.** Intermolecular energies of the compounds based on their rank.

| Compounds | Intermolecular energies or different poses ranked by energy (Kcal/mol) | | | | | | | | | | | |
|---|---|---|---|---|---|---|---|---|---|---|---|---|
| | 1 | 2 | 3 | 4 | 5 | 6 | 7 | 8 | 9 | 10 | Mean | SD |
| S1 | −0.59 | −0.48 | −6.31 | −6.21 | −6.12 | −6.11 | −5.9 | −5.77 | −5.53 | −5.52 | −4.85 | 2.29 |
| S2 | −7.56 | −7.4 | −7.13 | −6.73 | −6.62 | −6.5 | −6.15 | −5.96 | −5.91 | −5.71 | −6.56 | 0.64 |
| S3 | −8.11 | −7.62 | −7.21 | −7.01 | −6.91 | −6.9 | −6.88 | −6.53 | −6.23 | −5.84 | −6.92 | 0.64 |
| ML345 | −1.58 | −1.73 | −7.02 | −6.97 | −6.86 | −1.75 | −1.7 | −1.73 | −5.84 | −5.41 | −4.05 | 2.53 |

**Table 6.** Hydrogen bond interaction between insulysin and the different ligands.

| Pose | S1 | | S2 | | S3 | | ML345 | |
|---|---|---|---|---|---|---|---|---|
| | No. of H. bonds | Interacting residues | No. of H. bonds | Interacting residues | No. of H. bonds | Interacting residues | No. of H. bonds | Interacting residues |
| 1 | 2 | ARG429, SER435 | 2 | ILE624, GLN762 | 0 | – | 1 | Asn139 |
| 2 | 0 | – | 1 | GLN762 | 1 | ALA198 | 1 | Lys 217 |
| 3 | 1 | VAL1008 | 2 | ILE624, GLN762 | 1 | PRO897 | 1 | Ser 835 |
| 4 | 0 | – | 0 | – | 0 | – | 1 | Glu 290 |
| 5 | 1 | ILE624 | 1 | PHE459 | 1 | GLN111 | – | – |
| 6 | 2 | GLN111, ARG824 | 0 | – | 0 | – | 1 | Val833 |
| 7 | 0 | – | 0 | – | 0 | – | – | – |
| 8 | 1 | TRP495 | 2 | GLU156, GLU159 | 1 | VAL1008 | 1 | Asn43 |
| 9 | 1 | LYS217 | 2 | ASN43, ILE50 | 2 | GLU408, GLU156 | – | – |
| 10 | 1 | SER484 | 2 | GLU287, GLU290 | 1 | THR526 | – | – |

energy of −6.56 ± 0.64 and −6.92 ± 0.64 kcal/mol, respectively, on average. The residues in the receptor of insulysin interacting with their ligands through hydrogen bonds are presented in Table 6. It is evident from the table that all the ligands form either one or two hydrogen bonds with insulysin. But ML345 had formed only one hydrogen bond in 5 out of the 10 different poses with the receptor that it binds to. The interactions between insulysin and the inhibitors are shown in Figure 4.

**Biological activity analysis**

The synthesized compounds were sketched in Chemsketch and the PAAS software product. The results of the created "mol" files are presented in Table 7. The Pa of both S1 and S2 appears to be higher than 0.7 with values of 0.788 and 0.775, respectively, as per PAAS' requirement, leaving S3 with a value of 0.65 Besides, very small Pi (pharmacological inactivity) values are observed for all three compounds with S1 and S2 having values of 0.004, respectively, and S3 having a value 0.016. The synthesized compounds were tested for their drug-like properties using Molinspiration Webserver. The results of acquiescence of Lipinski's rule (the parameter designed by Pfizer in determining the "drug-likeness" of a compound) by all three compounds are depicted in Table 2. The molecular weight of all the three compounds range between 255.27 and 287.27 Da which is convincingly within the threshold of 500 Da as per Lipinski's rule. Similarly, the lipophilicity or hydrophobicity measure, logP, falls within 2.72 being not more than 5, in compliance with the Lipinski rule of 5. In the same way, the hydrogen bond donors are all lower than five and hydrogen bond acceptors are all lower than 10. On the contrary, the negative drug-likeness score (−1.44) for the compound S3 in comparison with the positive

values of compounds S1 and S2 is a prudence that it needs more investigation.

Having the Pa (pharmacological activity) values of 0.788 and 0.775, which exceeds 0.7, both S1 and S2 are very likely to exhibit a high potential in being a candidate as an inhibitor of insulysin, whose chances of being the analogue of a known pharmaceutical agent is promising. Along with this finding, S3 having a value of 0.65 slightly lower than 0.7 is likely to exhibit the activity in the experiment, but the probability of having similarity of a known pharmaceutical agent is unlikely. Besides, very small Pi (pharmacological inactivity) values obtained for all three compounds with S1 and S2 having 0.004, respectively, and S3 having a value of 0.016 indicates the prediction of the compound's efficacy to be evident, although S3 is of lesser extent (Rollas and Küçükgüzel, 2007). The drug-likeness property in accordance with the Lipinski rule of five by Pfizer were highly complied by the drug candidate in terms of the molecular mass, partition coefficient, hydrogen bond acceptor, and hydrogen bond donor, whose range of values falls within the proposed criteria (Lagunin *et al.*, 2010). The candidate compound is inclined toward lower molecular weight and lipophilicity, also complying with the extended rule of three (RO3) in defining lead-like compounds which will serve medicinal chemists an easier time in delivering of the optimized drug development candidates beside being drug-like (Chigurupati, 2015). However, the negative drug-likeness score (−1.44) for compound S3 in comparison to the positive values of compounds S1 and S2 is a prudence that it needs more investigation. Besides, when binding free energy was assessed against the stability of the compounds, there were evidence of higher stability in both S2 and S3 with binding free energy values of −5.97 ± 0.64 and −5.73 ± 0.64 Kcal/mol, respectively, when compared to S1 with a higher value of −4.86
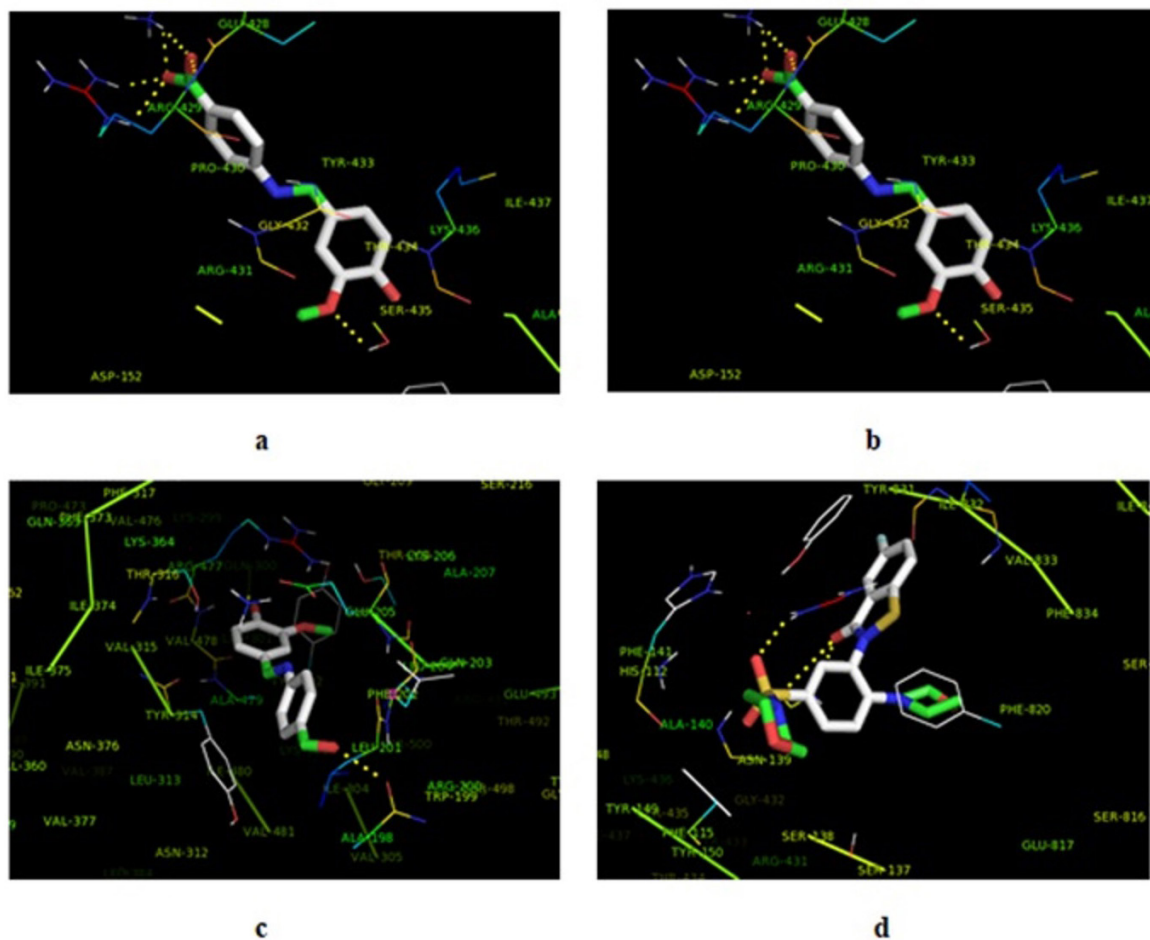
**Figure 4.** The interactions between insulysin and the inhibitors (a: Ligand S1; b: Ligand S2; c: Ligand S3; d: ML345).

**Table 7.** Biological activity prediction for the synthesized compounds.

| Compound | Structure | Molecular formula | Activity | Pa | Pi |
|---|---|---|---|---|---|
| S1 |  | $C_{15}H_{13}NO_4$ | Insulysin inhibitor | 0.788 | 0.004 |
| S2 |  | $C_{15}H_{13}NO_3$ | Insulysin inhibitor | 0.775 | 0.004 |
| S3 |  | $C_{15}H_{13}NO_5$ | Insulysin inhibitor | 0.650 | 0.016 |

± 0.37. In addition, ligands S2 and S3 having a lower binding free energy than the reported inhibitor (ML345) demonstrate a potential of being desired compounds in terms of molecular affinity, as lower energy level places the compound in a state of experiencing lesser shielding effect (less electron–electron repulsion) between both the binding entities. Nonetheless, being lower in energy gives the product a higher chance of being formed spontaneously in a chemical reaction than products of higher energy under the same conditions, due to the resultant kinetic stability at the time of bonding (Nasab *et al.*, 2018). On the contrary, a higher binding energy implicates the occurrences of binding only at a higher value, i.e., only when the required energy is available, which would be a drawback for the compounds with comparatively higher binding energy values. In assessing of the inhibitory constant (Ki) toward evaluation, the potency of the potential insulysin inhibitor M2 displayed the least inhibitory constant of 65.89 ± 58.24 μM, followed by S3 with 103.429 ± 115.44 μM leaving both these compounds to demonstrate lower inhibitory compounds when compared to ML345. Of note, having to do with the concentration required to reduce the activity of the specific enzyme, the inhibitory constant (Ki) reflects the binding affinity, while the half maximal inhibitory concentration (IC$_{50}$) is more reflective of the functional strength of the inhibitor for a drug. A competitive or uncompetitive inhibition pattern ascribes a Ki of about one-half of the value of the IC$_{50}$. This implies that a smaller Ki indicates a greater binding affinity and a lower concentration of drug needed in order to inhibit the activity of that enzyme (Anastas and Kirchhoff, 2002), suggesting both ligands S2 and S3 are more potent than compounds ML345 and S1 (325.36 ± 205.05 μM), making them good leads for designing insulysin inhibitor and aiding in controlling type 2 diabetes. Based on the intermolecular forces of the compounds, S1 appears to spearhead S2, S3, and ML345; however, the presence of more than one hydrogen bond involving all ligands S1, S2, and S3 only indicates the stability of the different binding poses as hydrogen bonding interacting plays a crucial role in the stabilization of supramolecular aggregates and also in the determination of the structure and stability of the 3-D structure adopted by macromolecules like proteins (Kastritis and Bonvin, 2013).

## CONCLUSION

4-Hydroxy-3-methoxybenzaldehyde Schiff bases were successfully prepared by the process of green synthesis and were found to be time-saving and environmentally friendly compared to the traditional synthetic technique. Due to the insulin-degrading function of the test compounds, it is reasonable to acknowledge their contribution for the stabilization of insulin levels as a therapeutic option in treating T2DM. Nevertheless, attention should be given to S2 as it held promising potential throughout all analytical data. S1 and S3 hold relatively convincing potential as drug candidate; however, being slightly inferior to S2 in all the analytical data, it is of prudence in requiring an in-depth investigation. With convincing prospect in the synthesis of S2 as an IDE, it may emerge as a promising lead compound in the venture of reversing the negative impact of T2DM on overall quality of life.

## AUTHOR CONTRIBUTIONS

All authors made substantial contributions to conception and design, acquisition of data, or analysis and interpretation of data; took part in drafting the article or revising it critically for important intellectual content; agreed to submit to the current journal; gave final approval of the version to be published; and agree to be accountable for all aspects of the work. All the authors are eligible to be an author as per the international committee of medical journal editors (ICMJE) requirements/guidelines.

## FUNDING

## CONFLICTS OF INTEREST

The authors report no financial or any other conflicts of interest in this work.

## ETHICAL APPROVALS

This study does not involve experiments on animals or human subjects.

## PUBLISHER'S NOTE:

This journal remains neutral with regard to jurisdictional claims in published institutional affiliation.

## REFERENCES

Ampofo AG, Boateng EB. Beyond 2020: modelling obesity and diabetes prevalence. Diabetes Res Clin Pract, 2020; 167:108362.

Anastas PT, Kirchhoff MM. Origins, current status, and future challenges of green chemistry. Acc Chem Res, 2002; 35:686–94.

Bendale AR, Bhatt R, Nagar A, Jadhav AG, Vidyasagar G. Schiff base synthesis by unconventional route: an in novative green approach. Der Pharm Chem. 2011; 3(2):34–8.

Berman HM, Westbrook J, Feng Z, Gilliland G, Bhat TN, Weissig H, Bourne PE. The protein data bank. Nucleic Acids Res, 2000; 28:235–42.

Blakemore DC, Castro L, Churcher I, Rees DC, Thomas AW, Wilson DM, Wood A. Organic synthesis provides opportunities to transform rug discovery. Nat Chem, 2018; 10:383–94.

Chigurupati S. Designing new vanillin schiff bases and their antibacterial Studies. Journal of Medical and Bioengineering, 2015; 4: 363-366.

Chigurupati S, Shaikh SA, Mohammad JI, Selvarajan KK, Nemala AR, Khaw CH, Teoh CF, Kee TH. *In vitro* antioxidant and *in vivo* antidepressant activity of green synthesized azomethine derivatives of cinnamldehyde. Indian J Pharmacol, 2017; 49:229–35.

Chigurupati S, Sitansu SN, Dong KY, Kesavanarayanan KS, Sohrab AS, Jahidul IM, Appala RN. Inhibitory activities of α-glucosidase and α-amylase and their hypoglycaemic capability in the treatment of diabetes. EC Pharmacol Toxicol, 2019; 7(2):79–91.

Dagogo-Jack S. Primary prevention of type 2 diabetes: an imperative for developing countries. In Dagogo-Jack S (ed.). Diabetes mellitus in developing countries and underserved communities. Springer, Cham, Switzerland, pp 7–31, 2017.

Durham TB, Toth JL, Klimkowski VJ, Cao JX, Siesky AM, Alexander-Chacko J, Guo SY. Dual exosite-binding inhibitors of insulin-degrading enzyme challenge its role as the primary mediator of insulin clearance *in vivo*. J Biol Chem, 2015; 290:20044–59.

Farris W, Mansourian S, Leissring MA, Eckman EA, Bertram L, Eckman CB, Selkoe DJ. Partial loss-of-function mutations in insulin-degrading enzyme that induce diabetes also impair degradation of amyloid β-protein. Am J Pathol, 2004; 164:1425–34.

Gaidhane S, Mittal W, Khatib N, Zahiruddin QS, Muntode PA, Gaidhane A. Risk factor of type 2 diabetes mellitus among adolescents from rural area of India. J Family Med Prim Care, 2017; 6:600–4.

Gilbert BJ. Republished: the role of amyloid β in the pathogenesis of Alzheimer's disease. Postgrad Med J, 2014; 90:113–7.

Hardling JL, Pavkov ME, Magliano DJ, Shaw JE, Gregg EW. Global trends in diabetes complications: a review of current evidence. Diabetologia, 2019; 62:3–16.

Kastritis PL, Bonvin AM. On the binding affinity of macromolecular interactions: daring to ask why proteins interact. J R Soc Interface, 2013; 10:20120835.

Lagunin A, Filimonov D, Poroikov V. Multi-targeted natural products evaluation based on biological activity prediction with PASS. Curr Pharm Des, 2010; 16:1703–17.

Leissring MA, Malito E, Hedouin S, Reinstatler L, Sahara T, Abdul-Hay SO, May PS. Designed inhibitors of insulin-degrading enzyme regulate the catabolism and activity of insulin. PloS One, 2010: 5:e10504.

Lipinski CA. Lead-and drug-like compounds: the rule-of-five revolution. Drug Discov Today, 2004; 1:337–41.

Manolopoulou M, Guo Q, Malito E, Schilling AB, Tang WJ. Molecular basis of catalytic chamber-assisted unfolding and cleavage of human insulin by human insulin-degrading enzyme. J Biol Chem, 2009; 284:14177–88.

Mathers CD, Loncar D. Projections of global mortality and burden of disease from 2002 to 2030. PLoS Med, 2006; 3:e442.

Mirsky IA, Perisutti G. Effect of insulinase – inhibitor on hypoglycemic action of insulin. Science, 1955; 122:559–60.

Morris GM, Huey R, Lindstrom W, Sanner MF, Belew RK, Goodsell DS, Olson AJ. AutoDock4 and AutoDockTools4: automated docking with selective receptor flexibility. J Comput Chem, 2009; 30:2785–91.

Nasab RR, Mansourian M, Hassanzadeh F. Synthesis, antimicrobial evaluation and docking studies of some novel quinazolinone Schiff base derivatives. Res Pharm Sci, 2018; 13:213–21.

Neelakantan MA, Esakkiammal M, Mariappan SS, Dharmaraja J, Jeyakumar T. Synthesis, characterization and biocidal activities of some schiff base metal complexes. Indian J Pharm Sci, 2010; 72:216.

Prentki M, Nolan CJ. Islet β cell failure in type 2 diabetes. J Clin Invest, 2006; 116:1802–12.

Rollas S, Küçükgüzel SG. Biological activities of hydrazone derivatives. Molecules, 2007; 12:1910–39.

Tabassum S, Amir S, Arjmand F, Pettinari C, Marchetti F, Masciocchi N, Pettinari R. Mixed-ligand Cu (II)–vanillin Schiff base complexes; effect of coligands on their DNA binding, DNA cleavage, SOD mimetic and anticancer activity. Eur J Med Chem, 2013; 60:216–32.

Wild S, Roglic G, Green A, Sicree R, King H. Global prevalence of diabetes: estimates for the year 2000 and projections for 2030. Diabetes Care, 2004; 27:1047–53.

Ye J. Mechanisms of insulin resistance in obesity. Front Med, 2013; 7:14–24.